International Journal of Technology 11(3) 522-531 (2020)
Received March 2019 / Revised March 2020 / Accepted May 2020

International Journal of Technology

http://ijtech.eng.ui.ac.id

Catalytic Pyrolysis of Spirulina platensis Residue (SPR): Thermochemical Behavior and Kinetics

Siti Jamilatun[1], Budhijanto[2], Rochmadi[2], Avido Yuliestyan[3], Muhammad Aziz[4,6], Jun-ichiro Hayashi[5], Arief Budiman[2*]

[1]*Department of Chemical Engineering, Faculty of Industrial Technology, Universitas Ahmad Dahlan, Jalan Kapas 9, Yogyakarta 55166, Indonesia*
[2]*Department of Chemical Engineering, Faculty of Engineering, Universitas Gadjah Mada, Jalan Grafika 2, Yogyakarta 55284, Indonesia*
[3]*Department of Chemical Engineering, Faculty of Industrial Technology, Universitas Pembangunan Nasional "Veteran" Yogyakarta, Jalan SWK 104, Yogyakarta 55283, Indonesia*
[4]*Institute of Innovative Research, Tokyo Institute of Technology, i6-25, 2-12-1 Ookayama, Meguro-ku, Tokyo 152-8550 Japan*
[5]*Institute for Material Chemistry and Engineering, Kyushu University, Kasuga 816-8580 Japan*
[6]*Institute of Industrial Science, The University of Tokyo, 4-6-1 Komaba, Meguro-ku, Tokyo 153-8505, Japan*

Abstract. The pyrolysis characteristics of *Spirulina platensis* residue (SPR) with silica–alumina catalysts were investigated using thermogravimetric analysis (TGA). The effects of differing amounts of catalysts on thermochemical behavior and kinetics parameters (pre-exponential factor in Arrhenius equation [A] and activation energy [Ea]) were studied. The experiment was carried out from 30 to 1000°C at a heating rate of 20°C/min for the case of non-catalytic and catalytic pyrolysis (silica–alumina). For the catalytic pyrolysis, also of interest were the catalyst-to-SPR weight ratios of 1:1 and 1:2. The TGA curve and differential thermogravimetric peak analysis results suggest that the use of catalysts in pyrolysis (particularly at a catalyst-to-SPR weight ratio of 1:1) reduces both pyrolysis time and temperature range to 14.68 min and 230–555°C, respectively. The kinetic parameters were then calculated in a one-step global non-isothermal model and solved using a least squares method in MATLAB. The presence of catalyst was able to reduce Ea to the lowest value from 41.10 kJ/mol (without catalyst) to 40.77 kJ/mol (weight ratio of 1:2) and 39.46 kJ/mol (weight ratio of 1:1) in Zone 1. However, the increase of catalyst quantity was not in line with the increase of reaction rate constant (k) and resulted in reasonably low A of, respectively, 593.30, 406.31, and 266.37.

Keywords: Activation energy, Catalytic pyrolysis; Pre-exponential factor; Spirulina platensis residue

1. Introduction

By 2040, the world's energy demand is estimated to have increased by 56%, with fossil fuels still contributing about 80% of the required supply (Anggorowati et al., 2018). This expectation has motivated an acceleration of the utilization of renewable sources, including algae. Microalgae such as *Spirulina platensis* have tremendous potential to be converted as a renewable fuel (Pradana et al., 2018). After the removal of lipid content by extraction, biomass in the form of *Spirulina platensis* residue (SPR), used as a biofuel material, has the

*Corresponding author's email: abudiman@ugm.ac.id, Tel/Fax.: +62-274-902170
doi: 10.14716/ijtech.v11i3.2967

potential to be converted through a process of pyrolysis (Jamilatun et al., 2017a; Kusrini et al., 2018; Jamilatun et al., 2019a).

Generally, a biofuel derived from the pyrolysis of SPR exhibits several deficiencies, including the presence of high levels of oxygenous and nitrogenous compounds. However, these disadvantages can be overcome through the use of a catalyst to reduce the levels of oxygenous and nitrogenous compounds (Bui et al., 2016). One suitable catalyst for upgrading the bio-oil is silica–alumina, which is widely used to support the production of petrochemicals, chemicals, and energy. The Al_2O_3 can promote the formation of aromatic compounds, such as polycyclic aromatic hydrocarbons. And with its low acidity, SiO_2 can also help remove oxygenated compounds and inhibit the formation of coke on the catalyst thanks to the porous medium (Aho et al., 2013; Busca, 2019; Jamilatun et al., 2019c). Jamilatun (2019c) reported that the catalytic pyrolysis on SPR using a silica–alumina catalyst (surface area of 240.553 m^2/g, pore size of 3.3 nm, average pore volume of 0.199 cm^3/g, and SiO_2/Al_2O_3 of 1.71) could reduce oxygenated compounds 37.47% (without catalyst) to 12.82% (a decrease of 65.80%). Further investigation on the catalytic thermal decomposition of SPR is crucially demanded to accelerate the development of bio-oil production (Sunarno et al., 2018; Jamilatun et al., 2019b; Jamilatun et al., 2019c). Its kinetic analysis and the thermal decomposition mechanisms necessary to obtain pre-exponential factor (A) and the reaction kinetics constant (k) from catalytic pyrolysis are the critical tools for designing reactor developments for industrial-scale bio-oil production (Li et al., 2013).

One effective method of analyzing both thermal decomposition and reaction kinetics is thermogravimetry (TG). Thermogravimetric analysis (TGA) has become a proven technique for investigating the non-catalytic pyrolysis of algae, including *Chlorella* sp., *Tetraselmis suecica* (Kassim et al., 2014), *Spirulina* extraction wastes (Li et al., 2013; Jamilatun et al., 2017b), and *Sargassum* sp. (Kim et al., 2013). On the other hand, there is minimal research on catalytic pyrolysis using the TGA method with microalgae raw materials, but Jamilatun et al. (2017b) reported that analysis of thermal decomposition and pyrolysis reaction kinetics of SPR with TGA indicated that the activation energy (Ea) for the heating rate of 20°C/min for Zones 1 and 2 was 41.102 kJ/mol and 0.0001240 kJ/mol. However, there has been almost no research work conducted on thermochemistry and kinetics of catalytic pyrolysis reactions using TGA. For this reason, research on catalytic pyrolysis of SPR needs to be developed, particularly with regard to pyrolysis thermochemical behavior and kinetics.

Based on TGA data, reaction kinetics can be approximated using a one-step reaction model derived from the Flynn–Wall–Ozawa and Kissinger–Akahira–Sunose methods (Kassim et al., 2014; Quan et al., 2016). In this method, a one-stage global single-reaction model can be determined via various approaches, such as the distributed activation energy model (DAEM), the iso-conventional method from Vyazovkin (Marriott et al., 2016), and nonlinear least squares regression (Kim et al., 2013). To the best knowledge of the authors, there is no previous study on biomass kinetic reactions incorporating natural and straightforward processes. Hence, as an alternative to establishing a one-stage global single-reaction model, a reaction model using a least squares method and MATLAB simulation tools was developed in this study. The data of catalytic thermal decomposition characteristics of SPR in TGA are required to determine the reaction kinetics, and the kinetics data are necessary to design the pyrolysis equipment for bio-oil production (Kim et al., 2013; Kassim et al., 2014; Quan et al., 2016).

This paper discusses the characteristics of thermal decomposition using a silica–alumina (SiO_2/Al_2O_3) catalyst, including the extent of the catalyst's effect on SPR weight

reduction. This work uses TG and differential thermogravimetric (DTG) curves to obtain the temperature ranges for Stage I (drying), Stage II (pyrolysis), and Stage III (gasification). The kinetic reaction was calculated through a one-step global non-isothermal model and solved with a least squares fitting using MATLAB simulation.

2. Methods

2.1. Materials

Blue-green microalgae, *Spirulina platensis*, were extracted to produce algal oil and a solid residue. The built residue (SPR) was used as the raw material for this research. The wet SPR was initially dried at 70°C in an oven to a constant weight and then homogenized until its size reached about 0.105–0.177 mm. Analyses of the protein, lipid, and carbohydrate contents of the SPR sample, together with calorific value analysis, were performed at the Research and Development Center for Mineral and Coal Technology (TEKMIRA), Bandung, Indonesia (Jamilatun et al., 2017a).

The catalyst used in this research was SiO_2/Al_2O_3, obtained from PT PERTAMINA Balongan Indonesia. The specifications of the SiO_2/Al_2O_3 were: (i) the ratio of SiO_2/Al_2O_3 was 1.67, and (ii) based on the BET method, the pore had a surface area of 240.553 m^2/g, with a pore diameter of 3.3 nm and mean pore volume of 0.199 cm^3/g to the total pore volume, and the contents of Na_2O, K_2O, CaO, and Fe_2O_3 were 0.48%, 0.017%, 0.035%, and 0.282%, respectively. SEM-EDX analysis revealed that the SiO_2/Al_2O_3 catalyst comprised C, O, Al, and Si of 12.33, 55.73, 15.42, and 16.51 wt.%, respectively (Jamilatun et al., 2017b; Jamilatun et al., 2019c).

2.2. Methods and Analysis

2.2.1. Pyrolysis test with TGA and thermochemical behavior

Thermal decomposition was examined using a TG–DTA (Perkin Elmer Pyris Diamond) at Leather Technology Academy, Yogyakarta (Politeknik ATK Yogyakarta). The mass of SPR, including the catalyst mixture (1:1 and 1:2 ratios) for each experiment, was 4–8 mg. Heating was carried out at a temperature range of 30 to 1000°C, and a rate of 20°C/min in the presence of 20 mL/min nitrogen gas. The selected heating rate had been previously tested by Jamilatun et al. (2017a).

2.2.2. Kinetics analysis

The one-stage global single-reaction model was used to obtain the reaction rate constant (k), including A and Ea. Although the pyrolysis of SPR biomass includes various very complex reactions, they can be considered as a single overall reaction (Kassim et al., 2014), with the equation for the reaction given as (Agrawal and Chakraborty, 2013)

$$\text{SPR} \rightarrow \text{Volatile matter} + \text{Char} \quad (1)$$

As shown in Equation 1, the pyrolysis with TG is non-isothermal, which can be observed as the change in SPR mass over time until the end of pyrolysis. The formed volatile matter mass could not be observed. The conversion change at any time (dX/dt) is affected by k, as the function of temperature (T), and conversion (f(X)) (Agrawal and Chakraborty, 2013).

$$dX/dt = k(T).f(X) \quad (2)$$

for,

$$f(X) = (1\text{-}X)^n \quad (3)$$

where n is the order of the reaction (this is assumed to be one). Moreover, the SPR conversion (X) is calculated using the following equation (Quan et al., 2016):

$$X = \frac{m_o - m_t}{m_o} \quad (4)$$

where X represents the conversion as a function of weight (m) from time 0 to time t. By initially providing the values of A, Ea, and universal gas constant (R) data, k can be calculated using

$$k = A.\exp\left(\frac{-E_a}{RT}\right) \quad (5)$$

Combining Equations 2–5 results in

$$\frac{dX}{dt} = A.\exp\left(\frac{-E_a}{RT}\right)(1-X)^n \quad (6)$$

$$T = T_O + \beta(t) \quad (7)$$

$$\beta = \frac{dT}{dt} \quad (8)$$

where β is the heating rate (°C/s), T_0 and T are the initial temperature and the temperature at a given t (K), respectively.

The A and Ea were then validated using the least squares method. The sum of squared errors (SSE) was calculated using the method in Jamilatun et al. (2017b):

$$SSE = \sum\{(X)_{model} - (X)_{data}\}^2 \quad (9)$$

3. Results and Discussion

3.1. Thermal Decomposition and Thermochemical Characteristics

The catalytic thermal decomposition characteristics of SPR were evaluated at a heating rate of 20°C/min in the presence of the SiO_2/Al_2O_3 catalyst. The results of the thermal decomposition for the catalyst-to-SPR weight ratios of 1:1, 1:2, and without catalyst can be seen in Figure 1, and the division of stages information is listed in Table 1.

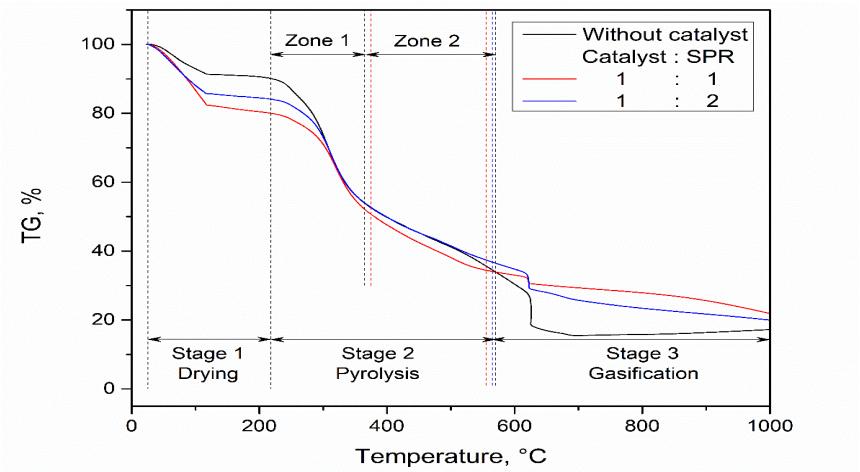

Figure 1 Thermal decomposition of SPR for the cases of the catalytic process with catalyst-to-SPR weight ratios of 1:1 and 1:2 and non-catalytic method at a heating rate of 20°C/min

The weight reduction of the SPR (obtained from the slope of the curve) can be seen in Figure 1. Catalytic and non-catalytic thermal decompositions exhibited a similar temperature range (30–230°C) in Stage I. Catalytic pyrolysis exhibited slight differences in

the temperature range for the ratios of 1:1 and 1:2, as shown in Table 1. The temperature ranges were 230–555°C and 230–565°C in Stage II, and 555–1000°C and 565–1000°C in Stage III, respectively. This temperature range contrasts with the non-catalytic pyrolysis, which exhibited a temperature range of 230–570°C in Stage II and 570–1000°C in Stage III. These phenomena may indicate that the catalyst reduces Ea; hence, the reaction proceeds more rapidly, resulting in faster pyrolysis (14.68 min) than without a catalyst (15.10 min).

Table 1 Division of stages upon catalytic and non-catalytic pyrolysis of SPR

Catalyst/SPR	1:1	1:2	Without catalyst
Stage I, °C (drying)	30–230	30–230	30–230
Stage II, °C (pyrolysis)	230–555	230–565	230–570
Stage III, °C (gasification)	555–1000	565–1000	570–1000
Pyrolysis time (Stage II), min	14.68	15.07	15.10

Furthermore, Stage II can be subdivided into two pyrolysis zones: Zone 1 (230–375°C for the 1:1 ratio and 230–365°C for the 1:2 ratio), with a rapid rate of weight reduction, and Zone 2 (375–555°C for the 1:1 ratio and 365–565°C for the 1:2 ratio), with a slower reduction rate. Meanwhile, for non-catalytic pyrolysis, Zones 1 and 2 ended at 350 and 570°C, respectively. Based on that, the use of a catalyst seems to affect the final temperature of the pyrolysis. In Zone 1, the final pyrolysis temperature with the catalyst (375°C) was higher than that without the catalyst (350°C), while in Zone 2, the temperature with the catalyst was lower (555°C) than that without the catalyst (570°C). Overall, without considering the presence of the pyrolysis zone, pyrolysis was achieved faster with the use of a catalyst, with a temperature range of 230–555 °C, as compared to without a catalyst at 230–570°C. This can be explained by the use of the catalyst possibly decreasing the activation energy so that it can accelerate the reaction, resulting in pyrolysis being achieved more quickly and in the lower temperature range.

DTG curves might be used to shed some light, based on the catalytic thermal decomposition of proteins and lipids, following the peaks summarized in Table 2 as a representation of the curves shown in Figure 2. The magnitude of the peak can describe the effect of temperature increase on the release of volatile matter (wt.%) for each time (min).

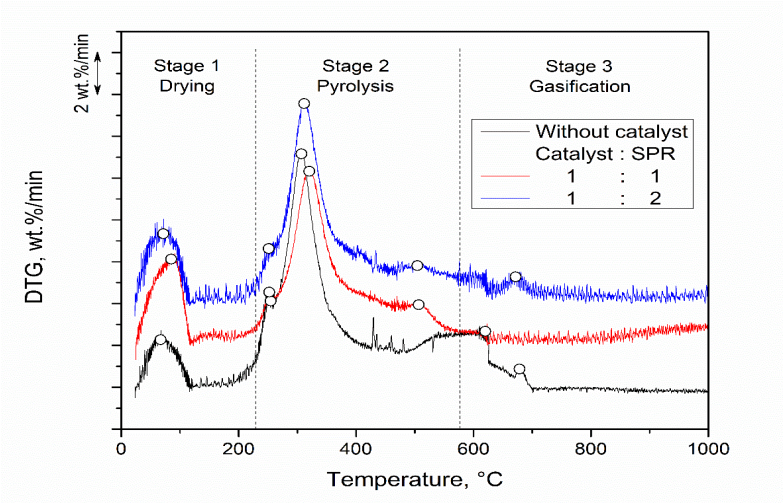

Figure 2 TG-DTG curve for catalytic thermal decomposition of SPR at a heating rate of 20°C/min: (a) the catalyst-to-SPR weight ratio of 1:1; (b) catalyst-to-SPR weight ratio of 1:2

From Figure 2, it can be observed that at a 20°C/min heating rate and 1:1 weight ratio, one peak was present in Stage I, three peaks were present in Stage II, and only one peak was present in Stage III. The evaporation of water (via O–H bond termination) occurred at 82.05°C at a rate of 4.35 wt.%/min. In the first zone of Stage II, two peaks were present at 262.30 and 318.05°C, with weight loss rates equal to 2.18 and 8.40 wt.%/min, respectively. Conversely, only one peak was observed in Zone 2, at 516.76°C, with a weight loss rate of 1.78 wt.%/min. The peaks in the pyrolysis zone indicate the release of volatile matter, meaning the decomposition of proteins and carbohydrates occurring through the termination of O–O, N–O, C–N, N–H, N=N, C=N, C–C, C=C, O=H, C–O, O–H, C=O, and C–H bonds. This phenomenon is the same as in a study by de Wild et al. (2011), showing that at the peaks in Zones 1 and 2, there is a breaking of the O–O, N–O, C–N, N–H, N=N, and C=N bonds with the decomposition of proteins, then a termination of C bonds C, C=C, and O=H bonds in cellulose decomposition, completion of C–C, C–O, O–H, C=O, and C–H bonds in hemicellulose decomposition, and termination of C bonds C, C=O and C–O in lignin decomposition.

Using a similar method applied to deduct the information in the 1:1 weight ratio case, peaks for non-catalytic thermal decomposition and catalytic decomposition at a 1:2 weight ratio were determined, and the results are shown in Table 2 and Figure 2b. For the non-catalytic process, a peak was observed at a similar position in Stage II, meaning in the temperature range where pyrolysis occurred. The volatile matter was released at a rate of 11.28 wt.%/min during non-catalytic decomposition at 305.62°C. Meanwhile, for catalytic decomposition, in summary, three peaks initially appeared at lower temperatures (253.95, 312.67, and 506.56°C) for the 1:2 ratio than for the 1:1 ratio (at 262.3, 318.05 and 516.77°C). However, the rates of volatile matter release with catalyst-to-SPR weight ratios of 1:1 and 1:2 were relatively similar, at 2.18–2.89, 8.40–9.78, and 1.78–1.83 wt.%/min.

Table 2 Peaks observed on DTG curves for catalytic and non-catalytic thermal decomposition of SPR at a heating rate of 20°C/min

Catalyst/SPR		Without catalyst	1:1	1:2
		Stage I (Drying)		
Peak 1	Temperature, °C	65.38	82.05	68.26
	DTG, wt.%/min	2.31	4.35	3.41
		Stage II (Pyrolysis)		
Peak 1	Temperature, °C	254.60	262.30	253.95
	DTG, wt.%/min	4.40	2.18	2.89
Peak 2	Temperature, °C	305.62	318.05	312.67
	DTG, wt.%/min	11.28	8.40	9.78
Peak 3	Temperature, °C	610.44	516.77	506.56
	DTG, wt.%/min	2.91	1.78	1.83
		Stage III (Gasification)		
Peak 1	Temperature, °C	681.08	618.83	675.65
	DTG, wt.%/min	0.97	0.51	1.45

3.2. Reaction Kinetics

The reaction kinetics of catalytic pyrolysis for the one-stage global single-reaction model can be derived from Equation 1, while the values of A and Ea can be calculated using Equations 2–5. By employing a least squares approach, the SSE calculation in MATLAB can be performed using Equation 9. The temperature (T) in Equation 8 is the pyrolysis temperature as influenced by time (t) and heating rate (β). Therefore, the relationship

between temperature (T_{data} and T_{model}) and pyrolysis time (t) in Zones 1 and 2 must be evaluated for the relative error. Evidence that the relative error is small can be observed in the selected experimental data for the catalyst-to-SPR ratio of 1:1; the results are presented in Figure 3a.

From Figure 3a, it can be observed that the line of temperature (T_{model}) versus time (t) in Zones 1 and 2 coincide with the scatter data (T_{data} vs. t). This relationship can be interpreted as evidence that the relationships between experimental data and models have the same relative values. Furthermore, the calculated conversion $(X)_{model}$ and the conversion observed in the experiment $(X)_{data}$ were employed to calculate the SSE using Equation 9. The relationship between both of these conversions with time (t) at a catalyst-to-SPR weight ratio of 1:1 can be seen in Figure 3b.

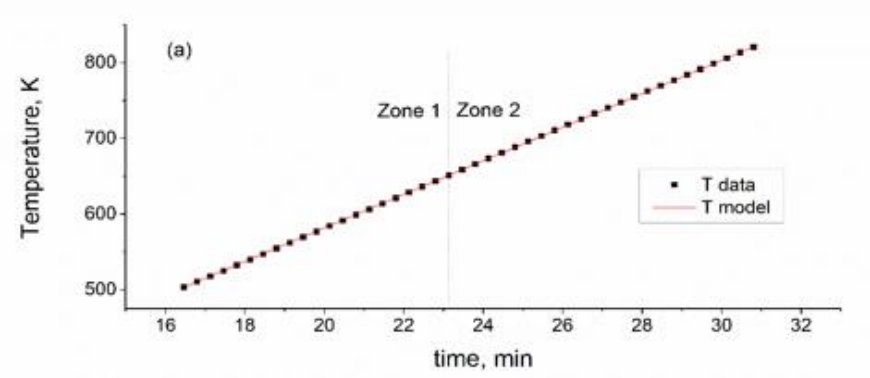

(a)

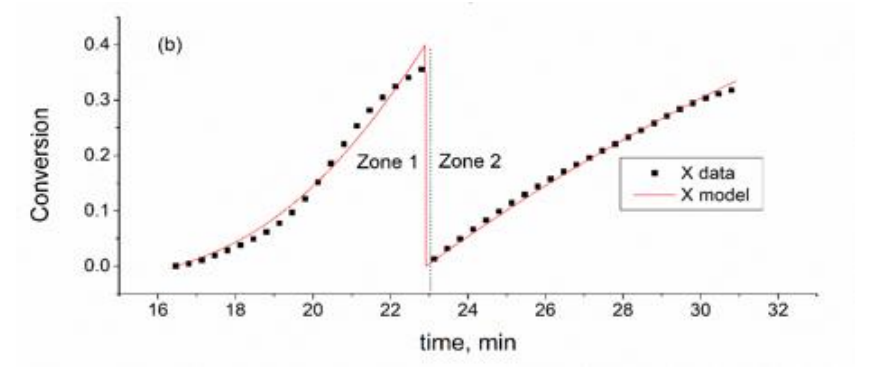

(b)

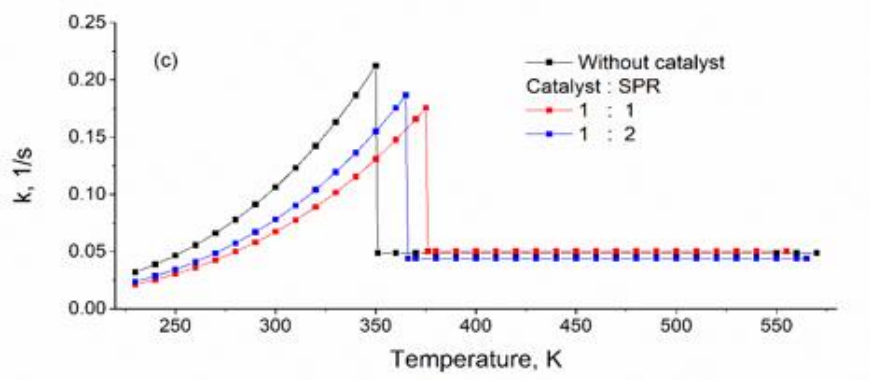

(c)

Figure 3 Kinetic parameters calculated for SPR pyrolysis at a heating rate of 20°C/min in Zones 1 and 2 for a catalyst-to-SPR weight ratio of 1:1: (a) relationship between time (t) and pyrolysis temperature (T); (b) relationship between time (t) and conversion (X); (c) relationship between the rate of reaction constant (k) and reaction temperature (T) with and without the catalyst

From the results of the simulation, with the values of A and Ea without and with a catalyst provided in Table 3, it can be observed that without the catalyst, A and Ea were 593.30 and 41.10 kJ/mol, respectively. In contrast, at a catalyst-to-SPR ratio of 1:1, these values became 266.37 and 39.46 kJ/mol, respectively, and at a catalyst-to-SPR ratio of 1:2, the values were 406.31 and 40.771 kJ/mol, respectively. The use of the catalyst decreased Ea due to the addition of new reaction pathways. Because catalytic pyrolysis is a very complex mechanism, the obtained Ea is affected by many reactions, including cracking, decarboxylation, decarbonylation, hydrocracking, hydrogenation, and hydrodeoxygenation (Purwanto et al., 2015; Supramono et al., 2015).

The decline of Ea can be interpreted as evidence that the catalytic pyrolysis reaction occurs more readily. In the calculation of k in Table 3 for Zone 1, it can be observed that with an increase of pyrolysis temperature, k rose accordingly. However, it appears that at a heating rate of 20°C/min and without the catalyst, the value of k is only slightly higher than with the catalyst. This is due to the shift in the final pyrolysis temperature range, meaning it shifts to higher temperatures; therefore, in the case without the catalyst, k is even higher than that with the catalyst (Kim et al., 2013; Marriott et al., 2016; Quan et al., 2016).

In addition, Table 3 also shows the calculated data for A, Ea, and k for Zone 2. It can also be observed that irrespective of the presence of a catalyst, the value of A is relatively similar. In contrast, the Ea value with the catalyst (0.0552–0.0853 J/mol) is much lower than without the catalyst (0.1421 J/mol). The values of k with and without the catalyst are almost the same (in the range of 0.0488–0.0505 s^{-1}), indicating that the temperature rise does not affect the amount of k, yielding relatively stable k values. The value of Ea in Zone 2 is a composite Ea of many reactions during pyrolysis (Li et al., 2013).

Table 3 Reaction kinetic parameters of the SPR with and without the catalyst at a heating rate of 20°C/min for Zones 1 and 2

Catalyst/ SPR	A	Ea (kJ/mol)	SSE	Temperature range, (°C)		k (s^{-1}) low temp.	k (s^{-1}) high temp.
Zone 1							
Without	593.30	41.10	0.0506	230	350	0.0320	0.2124
1:2	406.31	40.77	0.1005	230	365	0.0237	0.1865
1:1	266.37	39.46	0.0924	230	375	0.0213	0.1755
Zone 2							
Without	0.0488	1.42×10^{-4}	0.0421	351	570	0.0488	0.0488
1:2	0.0440	5.52×10^{-5}	0.0298	365	565	0.0440	0.0440
1:1	0.0505	8.53×10^{-5}	0.0151	375	555	0.0505	0.0505

Table 3 lists the kinetic parameters, and the results are presented in Figure 3c, showing the relationship between the SPR pyrolysis temperature and k for the catalyst-to-SPR ratios of 1:1 and 1:2 in Zones 1 and 2. Both with and without the catalyst, at a heating rate of 20°C/min in Zone 1, k during the pyrolysis is relatively low (0.021248–0.212346 sec^{-1}), about one-third of that at a heating rate of 40°C/min (0.0759–0.6797 sec^{-1}) (Jamilatun et al., 2017a). The value of k with the catalyst is slightly lower (0.021248–0.175527 sec^{-1}) than that without the catalyst (0.031980–0.212346 sec^{-1}). As for Zone 2, the curves coincide with each other to show the same k value (0.044000–0.050449 sec^{-1}), which is not affected by temperature rise. Due to the influence of A, this value seems to be low (0.0440–0.0505 sec^{-1}). The small amount of k in Zone 2 indicates that mass transfer had begun to take effect. As observed, the presence of catalysts causes a reduction in Ea.

However, its reaction rate decreases due to the lower value of k, contributed by the decline of A. Such phenomena may indicate a reduction of the molecular collision because it is hindered by the presence of the catalyst.

4. Conclusions

This study evaluated TG-DTG analyses as a feasible method for determining SPR pyrolysis characteristics. The release of volatile matter, seen in the DTG curve as a sharp peak, was observed in non-catalytic pyrolysis. In contrast, volatile matter release was relatively similar in the presence of the catalyst. Based on TG-DTG data, the presence of catalyst was able to reduce the pyrolysis time and temperature range, with observed data of 230–570°C (15.10 min); 230–565°C (15.07 min), and 230–555°C (14.68 min) for the cases of no catalyst, catalyst-to-SPR weight ratio of 1:2, and catalyst-to-SPR weight ratio of 1:1, respectively. In the same case sequence, the kinetic study reported the reduction of activation energy in Zone 1 as 41.10, 40.77, and 39.46 kJ/mol. However, the pre-exponential factor supports also appeared lower, at 593.30, 406.31, and 266.37. The reduction of activation energy due to the use of the catalyst is not in line with the increase of k due to the quite low pre-exponential factor. However, the rate in Zone 2 was not significantly affected because the values of the kinetic parameters were rather small and relatively similar to one another, in the range of 8.53×10^{-5}–1.42×10^{-4} kJ/mol and 0.0505–0.0488 for each activation energy and pre-exponential factor, respectively.

Acknowledgements

The authors are very grateful to the Ministry of Research and Technology/National Agency for Research and Innovation of the Republic of Indonesia for financial support.

References

Agrawal, A., Chakraborty, S., 2013. A Kinetic Study of Pyrolysis and Combustion of Microalgae *Chlorella vulgaris* using Thermo-Gravimetric Analysis. *Bioresource Technology,* Volume 128, pp. 72–80

Aho, A., DeMartini, N., Pranovich, A., Krogell, J., Kumar, N., Eränen, K., Holmbom, B., Salmi, T., Hupa, M., Murzin, D.Y., 2013. Pyrolysis of Pine and Gasification of Pine Chars–Influence of Organically Bound Metals. *Bioresource Technology*, Volume 128, pp. 22–29

Anggorowati, H., Jamilatun, S., Cahyono, R.B., Budiman, A., 2018. Effect of Hydrochloric Acid Concentration on the Conversion of Sugarcane Bagasse to Levulinic Acid. *In:* IOP Conference Series: Materials Science and Engineering, Volume 299, pp 1–6

Bui, H-H., Tran, K-Q., Chen, W-H., 2016. Pyrolysis of Microalgae Residues–A Kinetic Study. *Bioresource Technology*, Volume 19, pp. 362–366

Busca, G., 2019. *Silica-Alumina Catalytic Materials: A Critical Review.* Catalysis Today, In Press, Corrected Proof

de Wild, P.J., Reith, H., Heeres, E., 2011. Biomass Pyrolysis for Chemicals. *Biofuels*, Volume 2(2), pp. 185–208

Jamilatun, S., Budiman, A., Budhijanto, B., Rochmadi, R., 2017a. Non-Catalytic Slow Pyrolysis of *Spirulina platensis* Residue for Production of Liquid Biofuel. *International Journal of Renewable Energy Research,* Volume 7(4), pp. 1901–1908

Jamilatun, S., Budhijanto, B., Rochmadi, R., Budiman, A., 2017b. Thermal Decomposition and Kinetic Studies of Pyrolysis of *Spirulina platensis* Residue. *International Journal of Renewable Energy Development,* Volume 6(3), pp. 193–201

Jamilatun, S., Budhijanto, B., Rochmadi, R., Yuliestyan, A., Budiman, A., 2019a. Effect of Grain

Size, Temperature and Catalyst Amount on Pyrolysis Products of *Spirulina platensis* Residue (SPR). *International Journal of Technology*, Volume 10(3), pp. 541–550

Jamilatun, S., Budhijanto, B., Rochmadi, R., Yuliestyan, A., Budiman, A., 2019b. Valuable Chemicals Derived from Pyrolysis Liquid Products of *Spirulina platensis* Residue. *Indonesian Journal of Chemistry*, Volume 19(3), pp. 703–711

Jamilatun S., Budiman, A., Anggorowati, H., Yuliestyan, A., Surya Pradana, Y., Budhijanto, B., Rochmadi, R., 2019c. Ex-Situ Catalytic Upgrading of *Spirulina platensis* Residue Oil using Silica Alumina Catalyst. *International Journal of Renewable Energy Research*. Volume 9(4), pp. 1733–1740

Kim, S-S., Ly, H.V., Kim, J., Choi, J.H., Woo, H.C., 2013. Thermogravimetric Characteristics and Pyrolysis Kinetics of Alga *Sagarssum* sp. Biomass. *Bioresource Technology,* Volume 139, pp. 242–248

Kassim, M.A., Kirtania, K., de la Cruz, D., Cura, N., Srivatsa, S.C., Bhattacharya, S., 2014. Thermogravimetric Analysis and Kinetic Characterization of Lipid-Extracted *Tetraselmis suecica* and *Chlorella* sp. *Algal Research*, Volume 6(Part A), pp. 39–45

Kusrini, E., Supramono, D., Degirmenci, V., Pranata, S., Bawono, A.A., Ani, F.N., 2018. Improving the Quality of Pyrolysis Oil from Co-firing High-Density Polyethylene Plastic Waste and Palm Empty Fruit Bunches. *International Journal of Technology*, Volume 9(7), pp. 1498–1508

Li, L., Zhao, N., Fu, X., Shao, M., Qin, S., 2013. Thermogravimetric and Kinetic Analysis of Spirulina Wastes under Nitrogen and Air Atmospheres. *Bioresource Technology*, Volume 140, pp. 152–157

Marriott, A.S., Hunt, A.J., Bergström, E., Thomas-Oates, J., Clark, J.H., 2016. Effect of Rate of Pyrolysis on the Textural Properties of Naturally Templated Porous Carbons from Alginic Acid. *Journal of Analytical and Applied Pyrolysis*, Volume 121, pp. 62–66

Quan, C., Gao, N., Song, Q., 2016. Pyrolysis of Biomass Components in a TGA and a Fixed-Bed Reactor: Thermochemical Behaviors, Kinetics, and Product Characterization. *Journal of Analytical and Applied Pyrolysis,* Volume 121, pp. 84–92

Purwanto, W.W., Supramono, D., Muthia, R., Firdaus, M.F., 2015. Effect of Biomass Types on Bio-Oil Characteristics in a Catalytic Fast Pyrolysis Process with a Ni/ZSM-5 Catalyst, *International Journal of Technology*, Volume 6(7), pp. 1069–1075

Pradana, Y.S, Masruri, W., Azmi, F.A, Suyono, E.A., Sudibyo, H., Rochmadi, R., 2018. Extractive-Transesterification of Microalgae *Arthrospira* sp. using Methanol-Hexane Mixture as Solvent. *International Journal of Renewable Energy Research*, Volume 8(3), pp. 1499–1507

Supramono, D., Devina, Y.M., Tristantini, D., 2015. Effect of Heating Rate of Torrefaction of Sugarcane Bagasse on Its Physical Characteristics. *International Journal of Technology*, Volume 6(7), pp. 1084–1093

Sunarno, S., Rochmadi, R., Mulyono, P., Aziz, M., Budiman, A., 2018. Kinetic Study of Catalytic Cracking of Bio-Oil over Silica-Alumina Catalyst. *BioResources,* Volume 13(1), pp. 1917–1929